Numerical simulation of fluid flow in the mushy zone under rotation magnetic field: influence of permeability

Haijie Zhang, Menghuai WU*, Yongjian Zheng, Andreas Ludwig, Abdellah Kharicha
Chair for Simulation and Modeling of Metallurgy Processes, Department of Metallurgy,
University of Leoben, A-8700 Leoben, Austria
E-mail: menghuai.wu@unileoben.ac.at

Keywords: fluid flow, permeability, macrosegregation, rotation magnetic field

Abstract: A series of directional solidification experiments on Al-Si-M alloy were performed under terrestrial condition with RMF (rotation magnetic field) stirring [Kovács *et at.*, Materials Science Forum, 2010, 263-268]. Under a certain range of process parameters, a "Christmas tree" segregation pattern was observed. The current study is to use a two-phase columnar solidification model to simulate this segregation phenomenon, focusing on (1) its formation mechanism due to the RMF-induced interdendritic flow in the mushy zone; (2) the model sensitivity to different expressions of permeability law, as proposed by literatures. The geometry configuration for the calculation is identical with the sample (diameter of 8 mm) of the unidirectional solidification experiment, and the alloy is Al-7%Si alloy. Process parameters are taken from experiments. The agreements between calculated macrosegregation patterns and the experimental results are critically evaluated. In principle, the experimentally observed "Christmas tree" of macrosegregation can be numerically reproduced, if a correct permeability law with proper parameters is chosen under forced flow condition. The mushy zone thickness decreases with the increase of permeabilities. The formation of "Christmas tree" macrosegregation can be analyzed by the flow-solidification term ($\vec{u}_\ell \cdot \nabla c$).

Introduction

The interaction between a developing mushy zone and the melt flow is still an unclear issue, which is responsible for the formation of macrosegregation and plays important role in the formation of microstructure. To investigate the interdendritic flow and its interaction with the microstructure and macrosegregation, a series of experiments related to the MICAST (Microstructure Formation in Casting of Technical Alloys under Diffusive and Magnetically Convection Condition) research, supported by ESA (Europe Space Agency) were performed on ground and in space [1-4]. With the increase of the magnetic induction or decrease of the cooling rate, a central channel enriched with Si transforms into a channel with a shape of "Christmas tree" [2, 4]. Qualitative explanation of this phenomenon was that the solute rejected from the dendrites was captured by multiply traveling vortices and can be brought back to the mushy zone [2]. A series of simulations related to the MICAST project were made to better understand the flow-solidification interaction during the unidirectional solidification process. Noeppel et al.[5] studied the effect of the RMF and TMF on macrosegregation during directional solidification of Al-based binary alloy, and they suggested that the channels formed at the junction of two meridional vortices in the liquid zone. Similar works were also done by Budenkova et al.[6]. A periodical structure along the sample adjacent to the central channel was presented. However, they found that the characteristic time correspond to a spatial branch was quite long when it was compared with the oscillations of the fluid flow. It seemed that there was no direct relationship between the formation of spatial branches and oscillations of the fluid flow. From the previous works, the formation of "Christmas tree" macrosegregation is not fully explained.

Currently, the two-phase model, developed by Wu et al. [7-9], is used to simulate the unidirectional solidification process of the binary Al-7%Si alloy both under RMF and nature convection. A 2D axisymmetric model is established. Fluid flow in the bulk liquid and mushy zone is calculated under different permeability laws/expressions. Finally, formation mechanism of channel segregation is discussed.

Simulation Settings

The two-phase volume average model was described elsewhere [7-9]. A 2D axisymmetric model is established to simulate the solidification phenomenon. As shown in Figure 1, the alloy solidifies directionally with an imposed cooling rate (0.16 K/s) and temperature gradient (G = 6000 K/m). An RMF inductor is installed outside the cylindrical crucible. The rotation magnetic field, with the frequency 50 Hz, magnetic induction 20 mT, is controlled with a switch. Owing to the large aspect ratio (H/R), where H is the height of the sample and R is the radius of the sample, an analytical approximation of the azimuthal component of the electromagnetically force is assumed to be valid (Eq. (1)).

$$\vec{F}_\theta = \frac{1}{2}\sigma\omega B^2 r\left(\frac{\omega R - \bar{u}_\theta}{\omega R}\right)\vec{e}$$

(1)

where $\vec{F}_\theta$ is the azimuthal component of the electromagnetic force (N), σ is the electrical conductivity of the melt ($3.65\times10^6\Omega^{-1}m^{-1}$), $\omega=2\pi f$ is angular frequency (314), B is the magnetic induction (0.02 T), r and R (4 mm) is the radial coordinate and the radius of the crucible, and $\vec{u}_\theta$ is the practical azimuthal velocity (m/s) at a radial coordinate r. The initial temperature of the liquid is set as 1490 K, and a prospective temperature gradient is obtained by a pre-treatment. For the material properties the reader is referred to [5, 10].

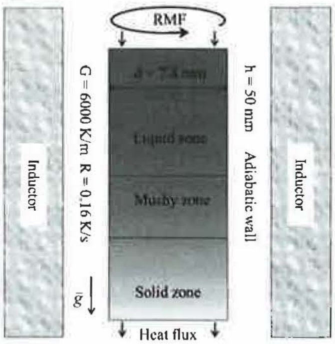

Figure 1. Geometry configuration and boundary conditions

Two laws of the isotropic permeability, derived from the Carman-Kozeny law and reported by Ramirez[11] and Noeppel [5], are employed in this part to evaluate the effect of the permeability on the fluid flow in the mushy. Noeppel's formulation (Eq.2) is related to λ_2, while Ramirez's formulation is related to λ_1 (Eq.3). Additionally, to cover the permeability range defined by different laws, two ultimate conditions, one is small enough and the other big enough, are considered. Details of four simulation cases are summarized in Table 1.

$$K = \frac{\lambda_1^2 f_\ell^3}{1667(1-f_\ell)^2} \quad (2) \qquad K' = \frac{\lambda_2^2 f_\ell^3}{4\pi^2 K_c(1-f_\ell)^2} \quad (3$$

Table 1. Permeability laws used for the current study

Cases	Expression	Relationship	Referred to	Parameters
a	-	$10K$	-	
b	$K' = \frac{\lambda_2^2 f_\ell^3}{4\pi^2 K_c(1-f_\ell)^2}$	$4K$	Noeppel [5]	$\lambda_1 = 300\mu m$ and $\lambda_2 = 50\mu m$, which are taken from experiments
c	$K = \frac{\lambda_1^2 f_\ell^3}{1667(1-f_\ell)^2}$	K	Ramirez [11]	
d	-	$0.1K$	-	

Simulation Results

As shown in Figure 2, meridional velocity and solute distribution are plotted for different cases. The vector stands for the liquid meridional velocity and the contour stands for mix solute concentration (c_{mix}). During the solidification process, when the RMF is on, an additional force is applied on the liquid phase. A large azimuthal velocity with the value of 0.13 m/s is generated under the current magnetic condition (20 mT), superimposed by the meridional circulation. The maximum meridional velocity is about 0.02 m/s, which is one order of magnitude smaller than the azimuthal velocity, but it is also four times larger than the velocity as induced only by buoyancy force. Some vortices are generated near the lateral wall and they move upward or downward, dissipating at the sample top surface or the solidification front. During the moving sequence of these vortices, some of the vortices aggregate to a big vortex. The generation and aggregation of these vortices seems randomly. The dissipation period of the vortex is about 1.5 s. Near the solidification front, two inward circulation flow pattern are observed. In the bulk liquid, the permeability of the mushy zone can hardly influence the velocity in the bulk liquid, so the flow pattern and flow intensity is very similar.

However, the segregation severity and the mushy zone thickness are highly dependent on the value of the permeability. In all cases, a central channel strongly enriched with the Si with a diameter of 1 mm is formed. Except for the case (a), all simulations present a "Christmas tree" segregation pattern adjacent to this central channel with periodical structure, which is consistent with the experimental result and other simulated result [2, 6]. A characteristic time for the periodical formation of channels is quite long (110 s), while the period of the vortex generation (1.5 s) is quite shorter. With the decrease of the permeability (from case a to case d), the segregation severity decreases significantly. Instead the formation of some channels, very strong negative segregation adjacent to the central positive segregation channel is observed in case (a).

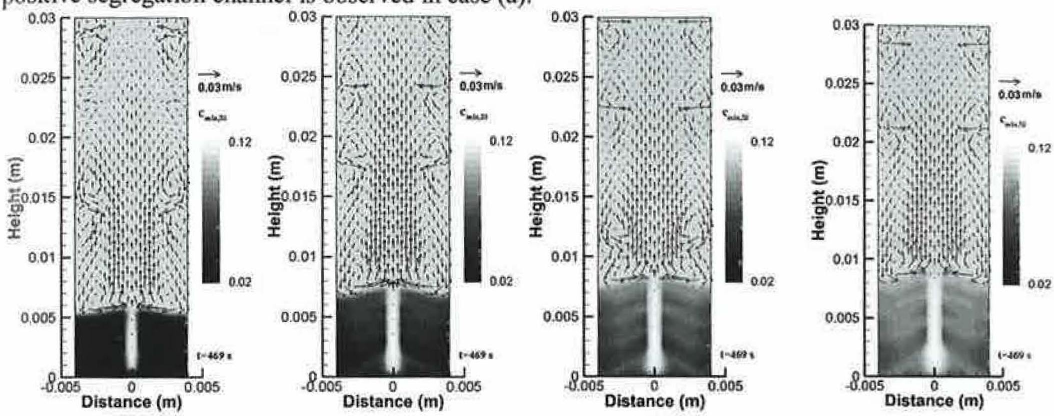

(a) (b) (c) (d)

Figure 2. Influence of the permeability of the mushy zone on the segregation pattern at 469 s: (a) $10K$; (b) $4K$; (c) K; (d) $0.1K$. Gray-scale shows c_{mix} with lighter showing higher concentration. Vector shows the liquid velocity in the bulk liquid. Maximum meridional liquid velocity in the bulk liquid is similar, $v_{max} = 0.02 m/s$.

The fluid flow in the mushy zone ($0 < f_\ell < 0.9$) is analyzed. As shown in Figure 3, the vector is the liquid velocity in the mushy zone and the solid line is the position of the eutectic temperature isotherm. Near the solidification front, the liquid volume fraction is lager and the magnitude of the liquid velocity is close to the velocity in the bulk liquid. In the deep mushy zone, the liquid velocity is weakened by the columnar dendrites, and the velocity there is two orders of magnitude smaller than that in the bulk liquid. The maximum permeability is employed in case (a), which means the lowest drag force applied on the liquid phase, leading to the biggest velocity in the mushy zone is observed. With the decrease of the permeability, the liquid velocity in the mushy zone is decreased obviously, which will suppress the solute transport in the mushy zone and reduce the segregation severity. Due to no channel formed in case (a), the velocity stream in mushy zone is very smooth, from the lateral region to the central channel. However, the velocity streams are contorted due to the formation of the channels in the case (b) to case (d), and solute-enriched liquid, rejected from the solid-liquid interface, is preferred to pass through these channels, and finally is washed into the central channel, which induces the positive segregation in the center part of the sample. The mushy zone thickness decreases with the increase of the permeability. The liquid velocity in the mushy zone is relative large when a large permeability is employed. The intensive liquid velocity in the mushy zone promotes the energy (enthalpy) transport. The hot liquid in the top of the mushy zone can be more easily transported to the deep part of the mushy zone, increasing the temperature gradient. This should be the reason for the decrease of the mushy zone thickness when increasing the permeability.

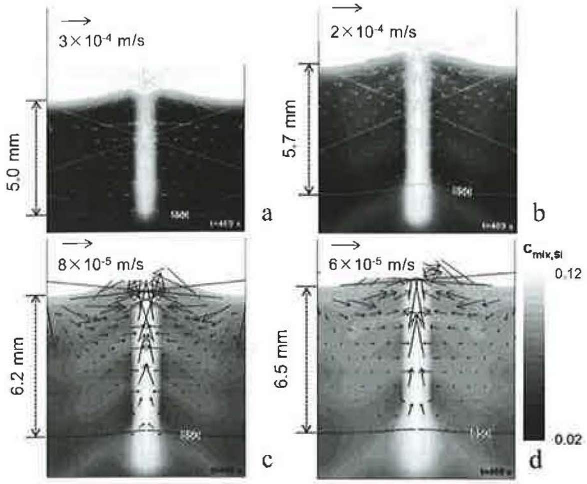

Figure 3. Influence of permeability on the fluid flow in mushy zone at 469 s: (a) $10K$; (b) $4K$; (c) K; (d) $0.1K$. Gray-scale shows c_{mix} with lighter showing higher concentration. Vector shows the liquid velocity in the bulk liquid. Solid line shows the position of the eutectic isotherm. Liquid velocity in the mushy zone decreases with the permeability.

Discussions

Formulation given by Li and Wu [8, 9] is employed to study the formation mechanism of channel segregation.

$$\frac{\partial(c_\ell^* - c_\ell)}{\partial t} = \frac{(c_\ell - c_s^*)}{f_\ell}\frac{\partial f_\ell}{\partial t} + \frac{1}{m}\frac{\partial T}{\partial t} + \vec{u}_\ell \cdot \nabla c$$

(4)

where f_ℓ is liquid volume fraction, c_ℓ is specie concentration in liquid phase, c_ℓ^* and c_s^* is interface equilibrium species concentration, and m is liquidus slope.

As shown in Eq. 4, the local solidification/melting rate is the result of three contributions, corresponding to the three right hand side (RHS) terms of Eq. (4). The first RHS term is the solidification induced solute enrichment of the interdendritic melt, which is always negative. The second RHS term is the contribution of the cooling rate, which is always positive. The third RHS term is the flow-solidification interaction term, which can be positive or negative depending on the interdendritic flow direction. Local solidification behavior highly depends on the sign of the flow-solidification interaction.

In a region where the melt flows in the same direction as the concentration gradient, the flow-solidification interaction term is positive. The local increase in the flow velocity due to a flow perturbation accelerates solidification and as a consequence of the locally permeability (K) becomes relatively smaller than that of neighboring zones and the interdendritic flow slows down, and channels do not form. On the contrary, in regions where the melt flows in the opposite direction of the concentration gradient, the flow-solidification interaction term is negative. The local increase in the flow velocity due to flow perturbation suppresses the solidification rate. This region with a relatively lower solid fraction has a larger permeability and the flow becomes stronger, and channels form.

As shown in Figure 4 (a), the vectors of liquid velocity and solute gradient are both plotted in gray and black respectively. When the angle between these two vectors is larger than 90°, the flow-solidification interaction term should be negative. The suppressed solidification zone, corresponding to negative $\vec{u}_\ell \cdot \nabla c$, is shown in Figure 4 (b), where the solidification rate was significantly slowed down, especially in the center channel zone. It can be seen that in the center zone of the sample, the flow-solidification interaction term is always negative, and the mass transfer is extremely lower than neighboring cells. Near the solidification front, which corresponds negative $\vec{u}_\ell \cdot \nabla c$, although the mass transfer rate is large, it should be suppressed currently. The suppressed solidification rate possibly leads to the formation of the channels. Once the channel forms, the liquid prefers to pass though these channel zone with the least resistance. As shown in Figure 4 (c), these regions, where channels form, with a relatively lower solid fraction, have a larger permeability and the enriched liquid is prefers to flow through the channel zone, which decreases the liquidus of the molten alloy, then the solidification process is further suppressed. This reinforced interaction will continue until the liquid is fully solidified. The final segregation pattern is shown in Figure 4 (d) by map and isolines, and the channel colored with black solid outline is the newly formed at 469 s.

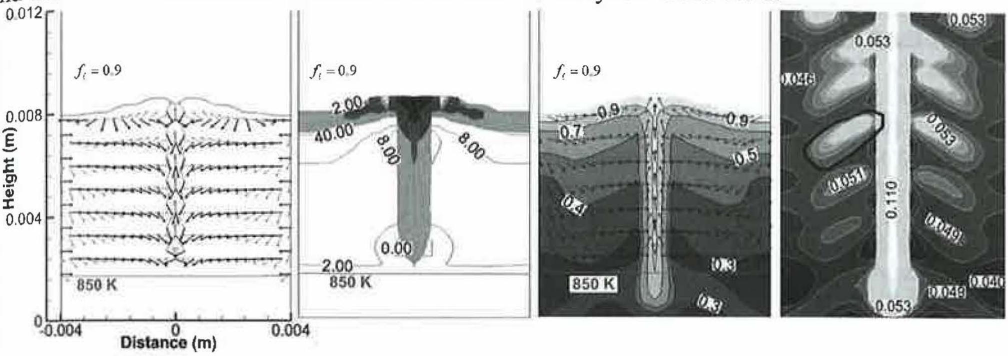

(a) (b) (c) (d)

Figure 4. Analysis of the formation of the channel segregation at t = 469 s: (a) vector of liquid velocity (gray) overlaid by vector c_{mix} (black); (b) contours of the flow-solidification interaction term ($\vec{u}_\ell \cdot \nabla c$) in white (positive) and black (negative) overlaid by the mass transfer rate ($M_{\ell c}$) isolines; (c) liquid volume fraction (f_ℓ) contours and isolines overlaid by vectors of liquid velocity; and (d) contour of c_{mix} and its isolines at 849 s. (Vector just stands for the direction in these figures)

Summary

A two-phase solidification model, coupled momentum, energy, species transfer is used to "reproduce" the unidirectional solidification process of Al-7%Si alloy under RMF (Rotation magnetic field). The fluid flow induced by the nature convection and RMF is consisted of a large azimuthal velocity superimposed with a meridional circulation. The meridional velocity is one order of magnitude smaller than the azimuthal velocity. Some vortexes randomly generate near the lateral wall and move to the crucible top and bottom. For the larger difference of the time magnitude, it seems that there is no direct relationship between the vortex generation and the channel formation, supporting Bodenkova et al.[2]. In principle, the experimentally observed "Christmas tree" of macrosegregation can be numerically reproduced, if correct permeability laws with proper parameters are chosen. The segregation severity is reduced when a smaller permeability is applied. The "Christmas tree" macrosegregation can be clearer if the permeability increases in a certain range. However, when the permeability value is extremely large, the "Christmas tree" of macrosegregation is replaced by the serious negative segregation. The mushy zone thickness decreases with the increase of the permeability. The formation of channels during the solidification process can be analyzed by the flow-solidification term ($\vec{u}_\ell \cdot \nabla c$).

References

[1] D. R. Liu, N. Mangelinck-Noël, C.A. Gandin, G. Zimmermann, L. Sturz, H.N. Thi, B. Billia, Structures in directionally solidified Al–7 wt.% Si alloys: Benchmark experiments under microgravity, Acta Mater., 64 (2014) 253-265.

[2] O. Budenkova, A. Noeppel, J. Kovács, A. Rónaföldi, A. Roósz, A.M. Bianchi, F. Baltaretu, M. Medina, Y. Fautrelle, Comparison between Simulation and Experimental Results of the Effect of RMF on Directional Solidification of Al-7wt.%Si Alloy, Mater. Sci. Forum, 649 (2010) 269-274.

[3] S. Steinbach, L. Ratke, G. Zimmermann, L. Sturz, A. Roosz, J. Kovács, Y. Fautrelle, O. Budenkova, J. Lacaze, S. Dost, Investigation of the effect of fluid flow on microstructure evolution in Al-Si-Fe alloys: The MICAST project, in: Decennial International Conference on Solidification Processing, 2017.

[4] J. Kovács, A. Rónaföldi, A. Roósz, Effect of the High Rotating Magnetic Field (min. 30 mT) on the Unidirectionally Solidified Structure of Al7Si0.6Mg Alloy, Mater. Sci. Forum 649 (2010) 263-268.

[5] A. Noeppel, A. Ciobanas, X.D. Wang, K. Zaidat, N. Mangelinck, O. Budenkova, A. Weiss, G. Zimmermann, Y. Fautrelle, Influence of Forced/Natural Convection on Segregation During the Directional Solidification of Al-Based Binary Alloys, Metall. Mater. Trans. B, 41 (2010) 193-208.

[6] O. Budenkova, F. Baltaretu, J. Kovács, A. Roósz, A. Rónaföldi, A.M. Bianchi, Y. Fautrelle, Simulation of a directional solidification of a binary Al-7wt%Si and a ternary alloy Al-7wt%Si-1wt%Fe under the action of a rotating magnetic field, in: Materials Science and Engineering Conference Series, 2012, pp. 012046.

[7] M. Wu, Y. Zheng, A. Kharicha, A. Ludwig, Numerical analysis of macrosegregation in vertically solidified Pb-Sn test castings – Part I: Columnar solidification, Comput. Mater. Sci., 124 (2016) 444-455.

[8] J. Li, M. Wu, J. Hao, A. Kharicha, A. Ludwig, Simulation of channel segregation using a two-phase columnar solidification model – Part II: Mechanism and parameter study, Comput. Mater. Sci., 55 (2012) 419-429.

[9] J. Li, M. Wu, J. Hao, A. Ludwig, Simulation of channel segregation using a two-phase columnar solidification model – Part I: Model description and verification, Comput. Mater. Sci., 55 (2012) 407-418.

[10] M. Ghods, L. Johnson, M. Lauer, R.N. Grugel, S.N. Tewari, D.R. Poirier, Radial macrosegregation and dendrite clustering in directionally solidified Al–7Si and Al–19Cu alloys, J. Cryst. Growth, 441 (2016) 107-116.

[11] J. C. Ramirez, C. Beckermann, Evaluation of a rayleigh-number-based freckle criterion for Pb-Sn alloys and Ni-base superalloys, Metall. Mater. Trans. A, 34 (2003) 1525-1536.